

→ *Electronic Supplementary Information for*

## Unusual similarity of DNA solvation dynamics in high-salinity crowding with divalent cations of varying concentrations

Deepika Sardana\*, Parvez Alam, Kavita Yadav, Ndege Simisi Clovis, Pramod Kumar and Sobhan Sen\*

Spectroscopy Laboratory, School of Physical Sciences, Jawaharlal Nehru University, New Delhi 110067, India

\*E-mails: dsardana92@gmail.com, sens@mail.jnu.ac.in

### Experimental Methods and Supplementary Data

**Materials:** The 14-mer HPLC purified palindromic DNA sequence, 5'-CGCGCAATTGCGCG-3' was from Integrated DNA Technology (IDT). DAPI (4', 6-diamidino-2-phenylindole, dilactate) was purchased from Sigma-Aldrich, and used as received. Double stranded DNA samples were prepared in respective ion's buffer solution at pH 7 by annealing. In the annealing process solution containing single stranded DNA heated at 95°C and then allowed to slowly cool to reach the room temperature (25°C) over ~6 hrs. In this work high and very high concentrations of two divalent ions, Mg<sup>2+</sup>, Ca<sup>2+</sup> of 0.15 M, 1 M, 2 M and monovalent, Na<sup>+</sup> of 0.15 M were used. This was achieved by adding requisite amounts of chloride salts of different cations to the corresponding buffer solution. For Na<sup>+</sup> 100 mM sodium phosphate buffer was used, added with 50 mM chloride salts (total Na<sup>+</sup> concentration is 0.15 M), while for Mg<sup>2+</sup> and Ca<sup>2+</sup>, 5 mM tris buffer with requisite amounts of chloride salts were added in DNA solution. HPLC grade (Merck) water was used in all sample preparation. The samples for steady-state and time-resolved fluorescence measurements were prepared with [DAPI]/[DNA] = 30 μM/300 μM, (ratio of 1:10), while for circular dichroism (CD) measurements the samples were prepared with either only ~6 μM DNA or 6 μM DNA with 6 μM DAPI.

**CD Spectroscopy:** The formation of B-form duplex-DNA structure was confirmed by CD spectra which were measured using a CD spectrometer (*Chirascan*, Applied Photophysics) (see Figure 2 in manuscript for the CD and induced CD-spectra. All experiments were performed at 26°C. Figure S1 plots the temperature dependent CD spectra of the DNA samples in respective concentrations of cations. The melting data show that ion-crowding by divalent cations decrease the DNA stability drastically, similar as found in UV-melting data below.

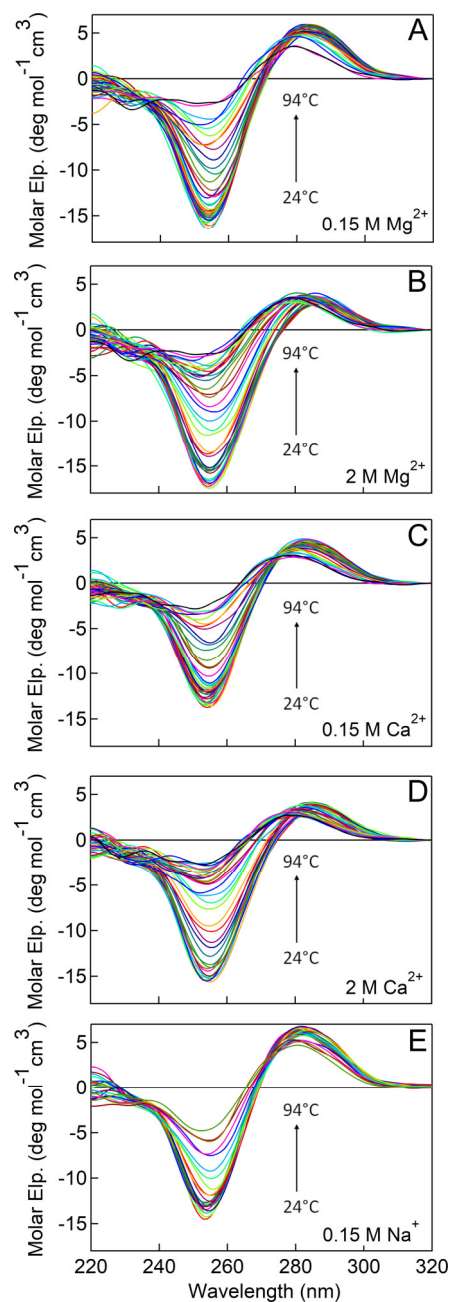


Figure S1. CD spectra of DNA at different temperatures in presence of different concentrations of cations. Temperature dependent CD spectra of DNA in presence of (A) 0.15 M  $\text{Mg}^{2+}$ , (B) 2 M  $\text{Mg}^{2+}$ , (C) 0.15 M  $\text{Ca}^{2+}$ , (D) 2 M  $\text{Ca}^{2+}$  and (E) 0.15 M  $\text{Na}^+$  See figure for legends.

**UV-Melting Data:** We measured absorbance change of DNA with temperature to measure the melting temperature of DNA samples, following the standard procedure.<sup>1,2</sup> A dual-beam JASCO V-670UV-vis-NIR spectrophotometer with Peltier controller (model no. ETCS 761) was used for measuring steady-state absorption spectra to obtain the melting profile of DNA in the presence of

Na<sup>+</sup> (0.15 M), Mg<sup>2+</sup> (0.15 M & 2 M) and Ca<sup>2+</sup> (0.15 M & 2 M). We recorded absorption spectra with change of 1°C temperature from 20°C to 90°C and monitored the absorbance change at 260 nm with respect to temperature. To calculate the melting temperature we analysed absorption data following standard reported procedure. Initially, we plotted the absorbance (260 nm) versus temperature, then calculated the linear function of temperature,  $A_L(T)$  and  $A_U(T)$  which represent the linear absorbance changes in the lower and higher range of temperatures, respectively. From this plot we calculated fraction of broken base pairs,  $\theta$  which is given by,<sup>1,2</sup>

$$\theta = \frac{A_T(T) - A_L(T)}{A_U(T) - A_L(T)} \quad (S1)$$

Here  $A_T(T)$  is the absorbance at various temperatures. Melting temperature is calculated at  $\theta = 0.5$ . Figure S2A plots the representative absorption data of DNA in the presence of 2 M Mg<sup>2+</sup> (only few data points are shown for clarity), and the absorbance at 260 nm plotted with temperatures, including the linear function of temperature  $A_L(T)$  and  $A_U(T)$  in Figure S2B. From this we calculated fraction of broken base pairs,  $\theta$  from equation S1 and melting temperatures from the value at  $\theta = 0.5$ . See Figure 2 and Table 1 in manuscript for the final results.

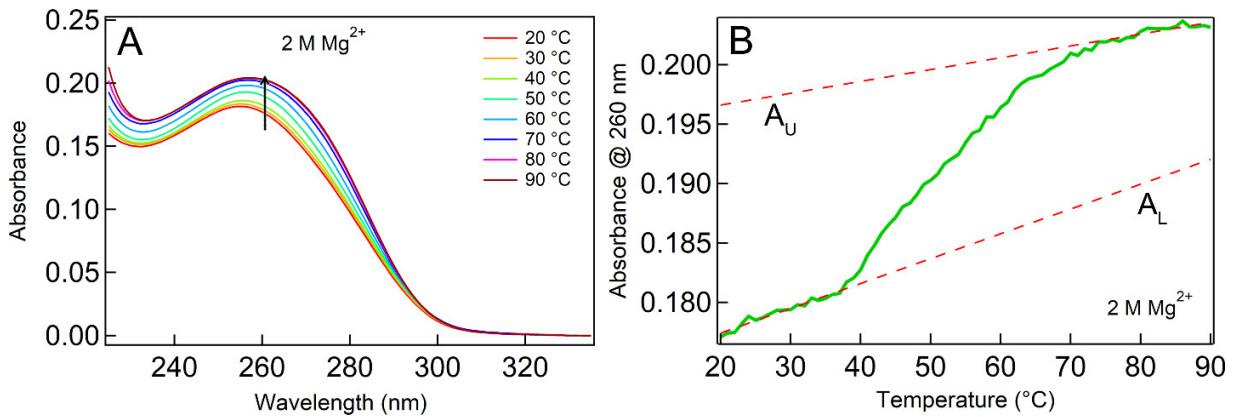


**Figure S2.** (A) Temperature dependent UV-melting spectra of DNA in presence of 2 M Mg<sup>2+</sup>. (B) Temperature dependent change in absorbance at 260 nm of DNA in presence of 2 M Mg<sup>2+</sup>.  $A_L(T)$  and  $A_U(T)$  represent the linear absorbance changes in the lower and higher range of temperatures which were subtracted from the raw UV-melting data to obtain the  $\theta$  vs. Temperature plot in Figure 2 according to equation S1.

**Fluorescence Spectra:** The fluorescence spectra were measured using a fluorescence spectrometer (Cary Eclipse, Agilent Technologies) using 5/5 nm band-passes of excitation and emission slits. Spectra were corrected using standard quinine sulfate spectrum.<sup>3</sup> The binding constants were measured using a highly sensitive fluorescence spectrometer (*FLS 920*, Edinburgh Instruments), by keeping the ligand (DAPI) concentration fixed at 10 nM and changing the DNA concentration from 1 nM to 30000 nM. Increment of the DNA concentration increases the fluorescence quantum yield of the DAPI due to higher binding to DNA minor groove. The binding

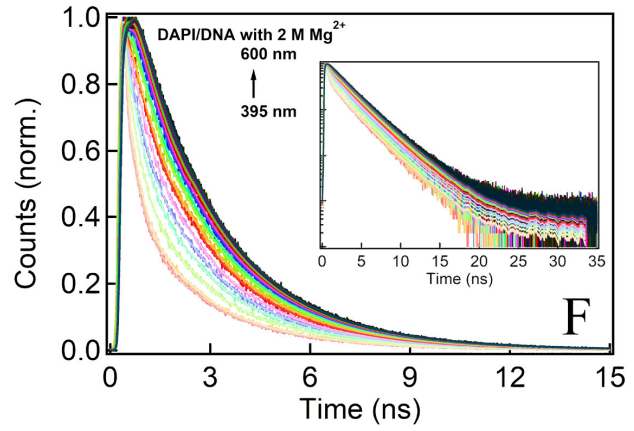
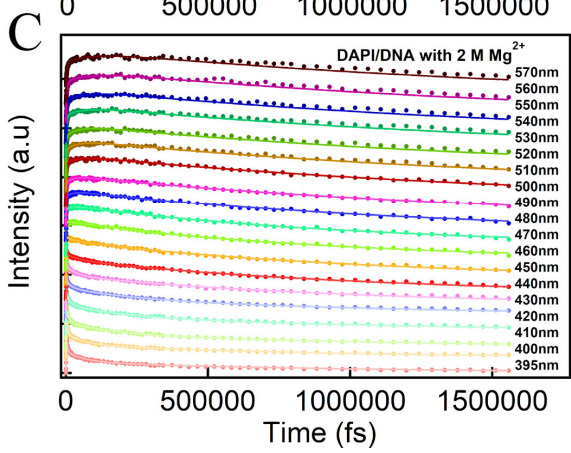
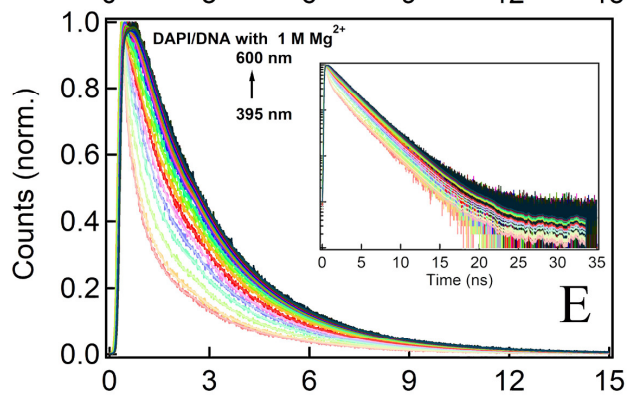
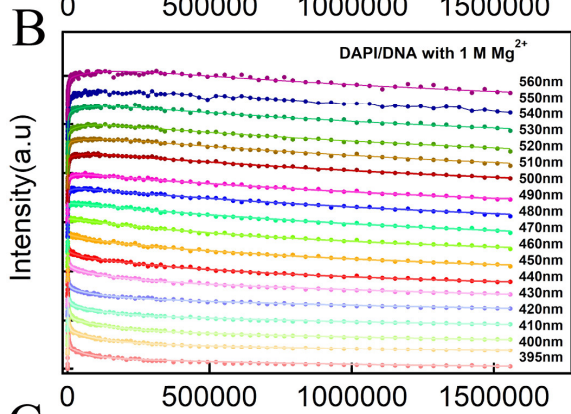
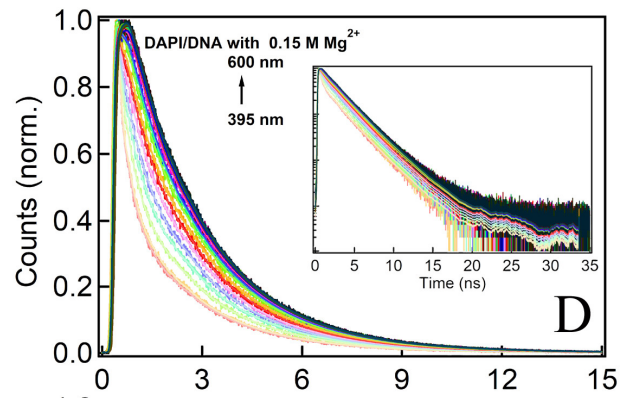
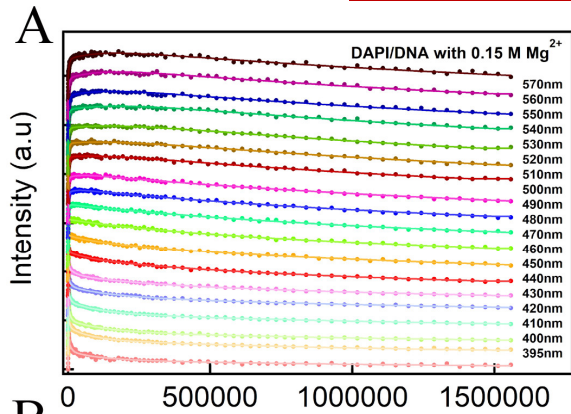
constants of DAPI to DNA in presence of respective cation concentrations were calculated by fitting of the relative fluorescence quantum yield data using equation S2.<sup>4,5</sup>

$$\Delta F = (\Delta F_{max}/2 \times C_t) \left[ \{[DNA] + [DAPI]_0 + (1/K)\} - \left\{ \sqrt{([DNA] + [DAPI]_0 + (1/K))^2 - (4 \times [DNA][DAPI]_0)} \right\} \right] \quad (S2)$$

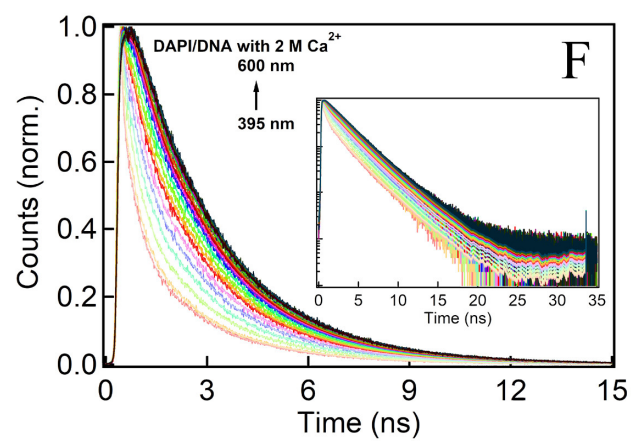
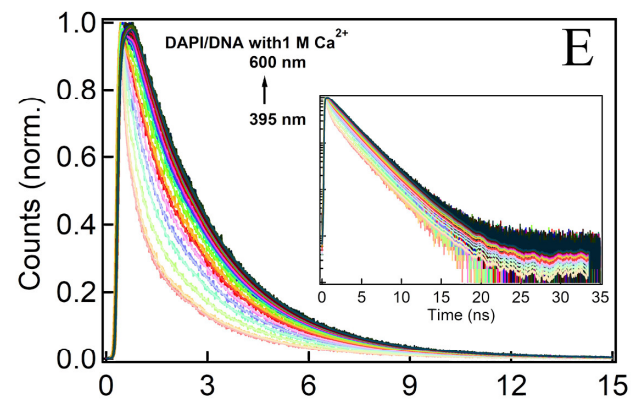
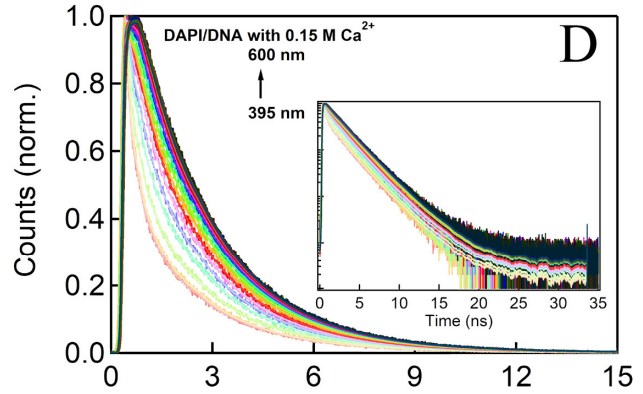
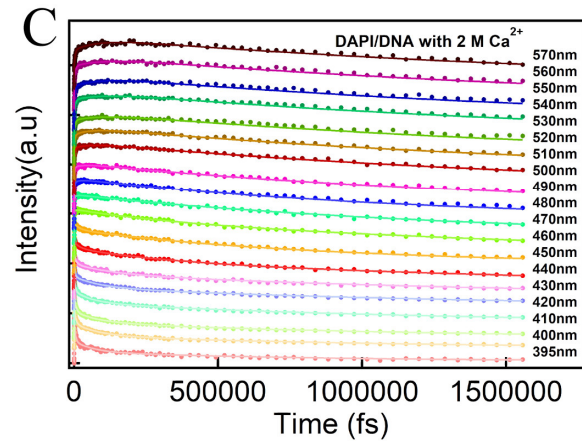
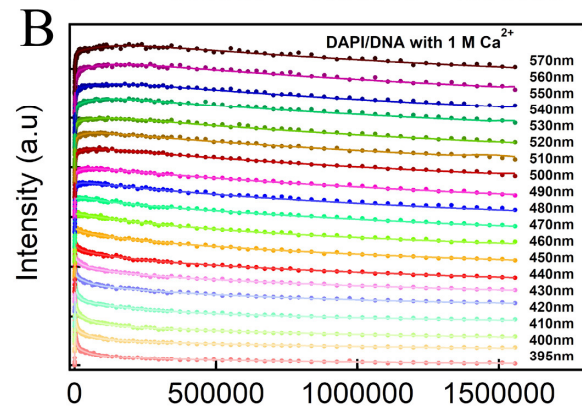
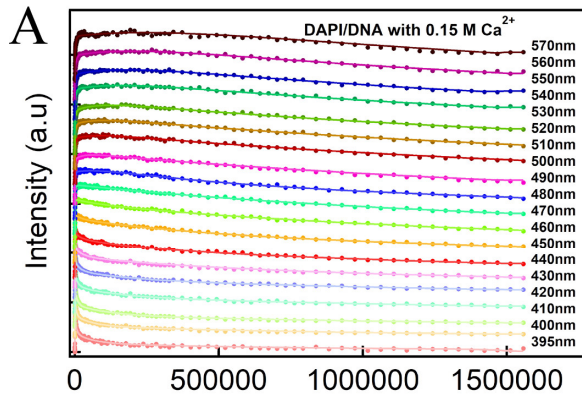
In above equation,  $\Delta F_{max}$  is the maximum quantum yield change of DAPI,  $C_t$  is total concentration of DAPI ( $\approx [DAPI]_0$ ),  $K$  is the binding constant, and  $[DNA]$  is the varying DNA concentration.

**Fluorescence Decay:** The fluorescence decays of DAPI/DNA complex from femtoseconds to nanosecond time-range were measured using femtosecond fluorescence optical gating (FOG) spectrometer (CDP Corp.), which was pumped with a Ti:Sapphire laser (MaiTaiHP, Spectra-Physics) of pulse-width of  $\sim 100$  fs and emission at 750 nm. Instrument response function (IRF) of FOG setup was  $\sim 250$  fs at 375 nm excitation. The decays in picoseconds to tens-of-nanoseconds time-scale were measured using time-correlated single photon counting (TCSPC) spectrometer (FLS-920, Edinburgh Instruments) with an excitation wavelength of 375 nm from a picosecond diode laser (Edinburgh Instruments). The IRF of TCSPC setup was  $\sim 110$  ps. All decays in FOG and TCSPC setups were measured at magic angle. Figure S3 plots the full sets of wavelength dependent decays measured in FOG and TCSPC setups. Wavelength dependent decays in FOG and TCSPC were measured covering the entire fluorescence spectrum from 395 nm to 600 nm for each DAPI/DNA samples at different cation concentrations of types. (Note that dynamic data for DAPI in 14-mer DNA in the presence of 0.15 M  $\text{Na}^+$  were also measured and reported in previous reports.<sup>6,7</sup> However, a new set of spectral data were again measured here for consistency and reproducibility.)

DAPI/DNA in different concentrations of  $Mg^{2+}$



DAPI/DNA in different concentrations of  $\text{Ca}^{2+}$



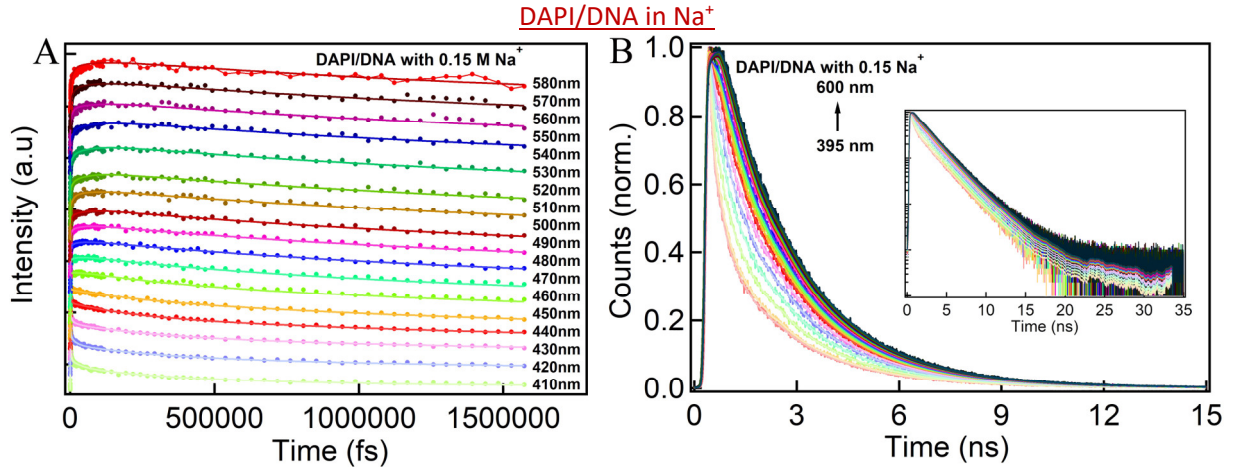


**Figure S3.** Fluorescence decays measured in the faster time-scale from femtoseconds to nanoseconds using FOG in different ionic conditions (left) and in slower time-scale using TCSPC in different ionic conditions (right). Plots also show multi-exponential fits (solid lines) through raw data points. The decays measured in FOG are shifted vertically from each-other for clarity. Insets in right panel show the complete TCSPC decays with fits.

**TRES Analysis and Dynamic Stokes Shift:** The fluorescence decays were fitted using sum of 3-4 exponentials through re-generative convolution of IRF and least-square fitting. Time-resolved emission spectra (TRES) were then constructed from the fitted parameters and normalized with respective fluorescence spectra of DAPI/DNA samples as,<sup>5</sup>

$$I(\bar{\nu}, t) = \frac{I_{ss}(\bar{\nu})}{\sum_{i=1}^n a_i \tau_i} \sum_{i=1}^n a_i e^{-t/\tau_i} \quad (\text{S3})$$

In equation,  $I_{ss}(\bar{\nu})$  is intensity of steady-state spectrum at a given wavenumber,  $\tau_i$  are time-components,  $a_i$  are amplitudes. TRES were constructed from 100 fs to 10 ns (see Figure 5 in manuscript for TRES of DAPI/DNA in presence of divalent cations and Figure S4 for TRES constructed for DAPI/DNA in presence of 0.15 M Na<sup>+</sup>). TRES were fitted with log-normal function and the dynamic fluorescence Stokes shifts from 100 fs to 10 ns were obtained in terms of 1<sup>st</sup> moment (mean) frequencies, calculated from the fits to TRES as,<sup>5</sup>

$$\bar{\nu}_1 = \frac{\int \bar{\nu} I(\bar{\nu}) d\bar{\nu}}{\int I(\bar{\nu}) d\bar{\nu}} \quad (\text{S4})$$

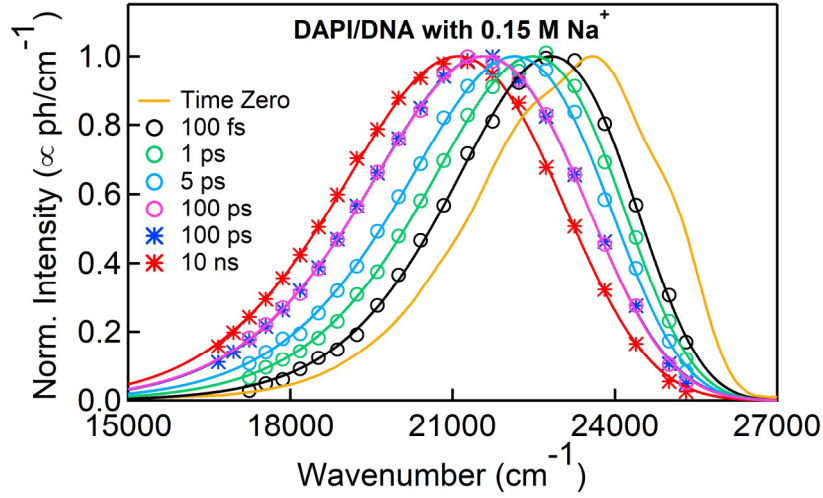


**Figure S4.** Normalized time-resolved emission spectra (TRES) of DAPI bound to DNA, constructed from the fitted parameters of fluorescence decays measured in FOG and TCSPC within the time-range from 100 fs to 10 ns in the presence of 0.15 M of  $\text{Na}^+$ . In spectra, line through points denote the lognormal fits to re-constructed TRES data. The plots also include time-zero glass spectra measured in the respective DAPI/DNA samples at low temperature (yellow solid line). The TRES obtained from FOG and TCSPC at common time-point (100 ps) show very good overlap.

**Time-Zero Glass Spectra:** The time-zero glass spectra of DAPI/DNA in respective salt-solutions were obtained as steady-state emission spectra of transparent glass samples prepared in glycerol/water mixture and measured in dry-ice/acetone mixture at  $-78^\circ\text{C}$  following procedures reported earlier<sup>5</sup> (see Figure 5 and Figure S4). To obtain the “absolute” Stokes shifts, the mean frequencies (equation S4) of TRES at room temperature were subtracted from the mean frequencies of steady-state glass spectra at low temperature for respective samples as (Figure 6),

$$S(t) = \bar{\nu}_1(\text{Time} - \text{Zero}) - \bar{\nu}_1(t) \quad (\text{S5})$$

**Anisotropy Decay:** Time-resolved fluorescence anisotropy of DAPI/DNA samples were measured by collecting the fluorescence decays at parallel and perpendicular emission polarizations, relative to vertical polarization of excitation (at 375 nm) using TCSPC setup at 460 nm emission (see Figure S5). Standard methods were used to calculate G-factor of TCSPC setup. The anisotropy decays were calculated using the decays measured at parallel and perpendicular polarizations as,<sup>5</sup>

$$r(t) = \frac{(I_{\parallel}(t) - GI_{\perp}(t))}{(I_{\parallel}(t) + 2GI_{\perp}(t))} \quad (\text{S6})$$



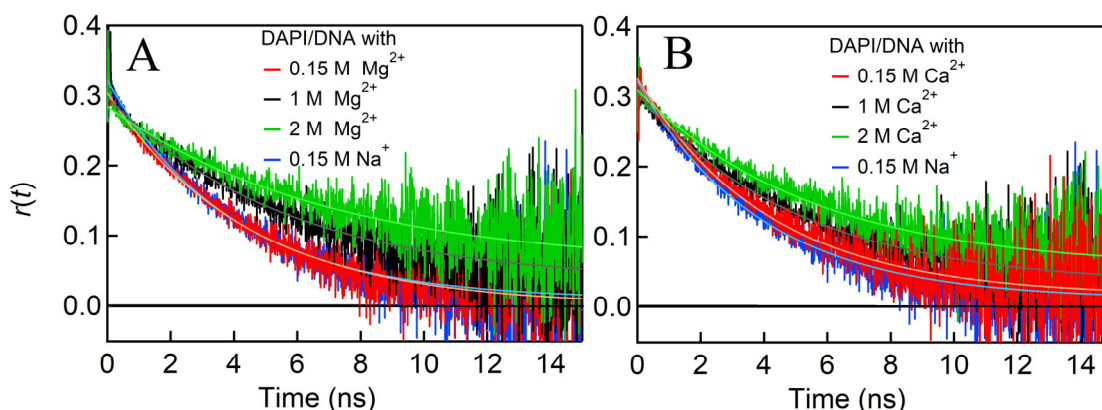


**Figure S5:** Fluorescence anisotropy decays of DAPI/DNA complex in presence of 0.15 M, 1 M and 2 M of (A)  $\text{Mg}^{2+}$  and (B)  $\text{Ca}^{2+}$ , along with their single exponential decay fits. In both plots the anisotropy decay of DAPI/DNA in presence of 0.15 M  $\text{Na}^+$  is also included for comparison. Data show higher concentrations of divalent cations introduce higher (micro) viscosity of the solution such that the anisotropy decay-time of DAPI/DNA get slower in hypersaline solutions.

### Supplementary References

- 1 R. M. Wartell and A. S. Benight, Thermal denaturation of DNA molecules: A comparison of theory with experiment, *Phys. Rep.*, 1985, **126**, 67–107.
- 2 R. Owczarzy, B. G. Moreira, Y. You, M. A. Behlke and J. A. Walder, Predicting stability of DNA duplexes in solutions containing magnesium and monovalent cations, *Biochemistry*, 2008, **47**, 5336–5353.
- 3 K. D. Velapoldi, R. A.; Mielenz, Standard reference materials. A fluorescence standard reference material: Quinine sulfate dihydrate, National Bureau of Standards, *Weber*, 1980, G 260–264.
- 4 S. Maiti, N. K. Chaudhury and S. Chowdhury, Hoechst 33258 binds to G-quadruplex in the promoter region of human c-myc, *Biochem. Biophys. Res. Commun.*, 2003, **310**, 505–512.
- 5 D. Sardana, K. Yadav, H. Shweta, N. S. Clovis, P. Alam and S. Sen, Origin of slow solvation dynamics in DNA: DAPI in minor groove of dickerson-drew DNA, *J. Phys. Chem. B*, 2019, **123**, 10202–10216.
- 6 S. D. Verma, N. Pal, M. K. Singh and S. Sen, Sequence-dependent solvation dynamics of minor-groove bound ligand inside duplex-DNA, *J. Phys. Chem. B*, 2015, **119**, 11019–11029.
- 7 N. Pal, S. D. Verma and S. Sen, Probe position dependence of DNA dynamics: Comparison of the time-resolved Stokes shift of groove-bound to base-stacked probes, *J. Am. Chem. Soc.*, 2010, **132**, 9277–9279.